
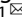



ARTICLE



The N⁶-methyladenosine writer WTAP contributes to the induction of immune tolerance post kidney transplantation by targeting regulatory T cells

Zhigang Wang^{1,3}, Yuanbo Qi^{1,3}, Yonghua Feng^{1,3}, Hongen Xu², Junxiang Wang¹, Luyu Zhang¹, Jie Zhang¹, Xinyue Hou², Guiwen Feng¹ and Wenjun Shang¹

© The Author(s), under exclusive licence to United States and Canadian Academy of Pathology 2022

N⁶-methyladenosine (m⁶A) modification is involved in diverse immunoregulation, while the relationship between m⁶A modification and immune tolerance post kidney transplantation remains unclear. Expression of Wilms tumor 1-associating protein (WTAP), an m⁶A writer, was firstly detected in tolerant kidney transplant recipients (TOL). Then the role of WTAP on regulatory T (Treg) cell differentiation and function in CD4⁺ T cells from kidney transplant recipients with immune rejection (IR) was investigated. The potential target of WTAP and effect of WTAP on immune tolerance in vivo were subsequently verified. WTAP was upregulated in CD4⁺ T cells of TOL and positively correlated with Treg cell proportion. In vitro, WTAP overexpression promoted Treg cell differentiation and enhanced Treg cell-mediated suppression toward naïve T cells. Forkhead box other 1 (Foxo1) was identified as a target of WTAP. WTAP enhanced m⁶A modification of Foxo1 mRNA in coding sequence (CDS) region, leading to up-regulation of Foxo1. Overexpression of m⁶A demethylase removed the effect of WTAP overexpression, while Foxo1 overexpression reversed these effects. WTAP overexpression alleviated allograft rejection in model mice, as evidenced by reduced inflammatory response and increased Treg population. Our study suggests that WTAP plays a positive role in induction of immune tolerance post kidney transplant by promoting Treg cell differentiation and function.

Laboratory Investigation (2022) 102:1268–1279; <https://doi.org/10.1038/s41374-022-00811-w>

INTRODUCTION

Transplantation of donor's kidney to non-human leukocyte antigen identical recipients induces alloimmune responses, clinically known as graft rejection, which strongly threatens the graft and patient survival¹. In recent years, the clinical application of allograft rejection post kidney transplantation has been reduced with the introduction of immunosuppressive regimens². However, the long-term administration of immunosuppressive drugs increased the risk of systemic infections and malignancies³. The major challenge of transplant medicine remains the induction of specific immune tolerance to allograft with minimal use of immunosuppressive drugs.

Regulatory T (Treg) cells, characterized by the expressions of CD4, CD25, and forkhead box P3 (Foxp3), are a subpopulation of CD4⁺ T cells that are closely related to the induction and maintenance of immune tolerance⁴. The numbers of peripheral CD4⁺CD25⁺Foxp3⁺ cells are lessened in kidney transplant patients with chronic rejection compared with operationally tolerant patients with stable graft function, indicating the involvement of Treg cells in immune tolerance post kidney transplantation⁵. Meanwhile, increasing studies confirm the effectiveness of inducing the immune tolerance post kidney transplant by manipulating Treg cells. The research of Pang et al.⁶ reported that immature dendritic cells promoted

immune tolerance in renal allograft model mice by promoting Treg cell differentiation. Wu et al.⁷ reported that a high-fiber diet induced Treg-dependent tolerance in a kidney transplant model by producing short-chain fatty acid. As reported, the differentiation, maintenance, and functional maturation of Treg cells are regulated by Foxp3⁸. Through stabilizing Foxp3 protein, Nemo-like kinase maintained Treg cell-mediated immune tolerance in vivo⁹. These previous evidence suggest that Foxp3 is a potential target for the regulation of Treg cell-induced immune tolerance post kidney transplantation.

N⁶-methyladenosine (m⁶A) is one of the most abundant and important RNA modifications in eukaryotes and regulates several aspects of RNA metabolism, including RNA decay, splicing, and translation. Regulators mediating the m⁶A function are divided into 3 types: methyltransferases, demethylases, and m⁶A binding proteins¹⁰. Methyltransferases, also terms as "writers", are responsible for the catalyzation of m⁶A modification. Demethylases, also terms as "erasers", are responsible for the removal of methylation. M⁶A binding proteins, also called "readers", recognizing and binding m⁶A sites, resulting in different destinies of target RNA¹¹. The research of Tong et al.¹² reported that deletion of methyltransferase-like 3 (METTL3, an m⁶A reader) in Treg cells deprived Treg suppression function, leading to severe

¹Department of Kidney Transplantation, The First Affiliated Hospital of Zhengzhou University, Zhengzhou 450000, China. ²Precision Medicine Center of Zhengzhou University, Academy of Medical Sciences, Zhengzhou University, Zhengzhou, China. ³These authors contributed equally: Zhigang Wang, Yuanbo Qi, Yonghua Feng
✉email: zhigang2012@126.com; fengguiwen@zzu.com.cn; shangwj111@163.com

Received: 10 November 2021 Revised: 27 May 2022 Accepted: 30 May 2022
Published online: 21 July 2022

autoimmune diseases in mice, suggesting that m⁶A modification is related to Treg cell function. In our preliminary experiment, the dataset Gene Expression Series (GSE) 22229 was downloaded from the Gene Expression Omnibus (GEO) database, and several m⁶A-related genes were dysregulated in tolerant kidney transplant recipients compared with kidney transplant recipients receiving standard immunotherapy. However, whether m⁶A modification participates in the induction of immune tolerance post kidney transplantation through modulating Treg cell function remains unclear.

In this study, we explored the role of m⁶A modification in immune tolerance post kidney transplantation for the first time, identified the specific m⁶A-related genes that regulated Treg cell differentiation and function, and elucidated the underlying mechanism.

MATERIALS AND METHODS

Data resource

The dataset GSE22229 (DOI:10.1172/JCI39933) was downloaded from the GEO database. The gene expression data were derived from the whole-blood samples from tolerant kidney transplant recipients (TOL, *n* = 19), kidney transplant recipients receiving standard immunotherapy (SI, *n* = 26), and healthy control subjects (non-transplanted; control, *n* = 13).

Patients

With the approval of the Ethics Committee of The First Affiliated Hospital of Zhengzhou University, tolerant kidney transplant recipients (TOL, *n* = 20) and kidney transplant recipients with immune rejection (IR, *n* = 20), and healthy control subjects (non-transplanted; HC, *n* = 20) were enrolled in this study. The whole-blood samples of all participants were collected in tubes containing anticoagulants after they signed informed consent forms. TOL was defined as possessing a stable graft function without immunosuppression for more than 1 year. IR was defined with graft dysfunction that showed signs of immunologically driven rejection despite adequate immunosuppression.

Isolation of human CD4⁺ T cells and naïve CD4⁺ T cells, and lentivirus infection

Human CD4⁺ T cells were isolated from the whole-blood samples of TOL, IR, and HC (healthy control) groups using Dynabeads[®] FlowComp[™] Human CD4 Kit (Thermo Fisher Scientific, Waltham, MA, USA). Whole-blood was incubated with FlowComp[™] Human CD4 Antibody for 10 min and FlowComp[™] Dynabeads[®] for 15 min. The mixture was washed with the Isolation Buffer and the supernatant was removed. Beads-bound CD4⁺ T cells were incubated with FlowComp[™] Release Buffer and placed in a magnet. The supernatant containing beads-free CD4⁺ T cells were then added with Isolation buffer and CD4⁺ T cells were collected by centrifugation at 350×g. Cells were cultured in Roswell Park Memorial Institute (RPMI)-1640 medium containing 10% fetal calf serum (FCS) and 1% penicillin-streptomycin solution at 37 °C with 5% CO₂. Human peripheral blood mononuclear cells (PBMCs) were isolated from peripheral blood of IR patients by Ficoll-Hypaque density-gradient centrifugation. Human naïve CD4⁺ T cells were isolated by using the EasySep[™] Human Naïve CD4⁺ T Cell Isolation Kit (STEMCELL Technologies, Beijing, China) followed the manufacturer's instructions.

Lentivirus (Lenti)-Wilms tumor 1-associating protein (WTAP), Lenti-forkhead box other 1 (Foxo1), and negative control (Lenti-control) were produced by Hanheng Biotechnology Co., Ltd (Shanghai, China). For lentivirus infection, human naïve CD4⁺ T cells were transferred to 24-well plate pre-coated with anti-human CD3 (5 µg/ml) and soluble anti-human CD28 (5 µg/ml) and stimulated by interleukin (IL)-2 (100 U/ml) for 48 h. Then, cells were incubated with the corresponding lentivirus with 100 multiplicity of infection and polybrene (6 µg/ml; Yeasen Biotechnology Co., Ltd., Shanghai, China). Six hours later, the medium containing lentivirus was replaced with the fresh complete medium and cells were cultured for another 72 h.

Analysis of Treg and CD4⁺ T cell population

To determine the population of Treg cells in CD4⁺ T cells sorted by dynabeads, cells were stained with phycoerythrin isothiocyanate (FITC) mouse anti-human CD25 and P-ained with fluorescein isothiocyanate (FITC) mouse anti-human CD25 and P-ained with fluorescein isothiocyanate (FITC) mouse anti-human Foxp3 (all purchased from BD Biosciences, San Jose, CA, USA). The ratio of CD25⁺ Foxp3⁺ cells was measured by flow cytometry.

To determine the population of CD4⁺ T cells in the spleen tissues of mice, single-cell suspension was generated from spleen tissues as previously described¹³, and the cells were stained with Percp anti-mouse CD4 (Biolegend, USA), PE anti-mouse CD25 (Biolegend), and APC anti-mouse Foxp3 (eBioscience, USA). The ratio of CD4⁺ T cells was measured by flow cytometry.

Treg polarization

Naïve CD4⁺ T cells generated from the IR group were transferred to plates pre-coated with anti-human CD3 (5 µg/ml) and soluble anti-human CD28 (5 µg/ml), and stimulated by IL-2 (100 U/ml) and TGF-β (5 ng/ml) for 72 h.

Treg cell suppression assay

Naïve CD4⁺ T cells generated from the IR group were infected with Lenti-WTAP or Lenti-control and then differentiated into Treg cells. Naïve CD4⁺ T cells (5 × 10⁴) generated from the IR group were labeled with 4 µM carboxyfluorescein diacetate succinimidyl ester (CFSE, Abmole Bioscience, Houston, TX, USA) and were cultured for 5 days in the presence of plate-bound anti-CD3 (5 µg/ml), soluble anti-CD28 (5 µg/ml) and an equal number of induced Treg cells. At the end of the culture, CFSE fluorescence was analyzed by flow cytometry. The proliferation of naïve CD4⁺ T cells was determined by calculating the division index of CFSE⁺ cells.

Quantitative real-time PCR (qRT-PCR)

Total RNA samples were isolated from cells and spleen tissues using a MolPure[®] Cell/Tissue Total RNA Kit (Yeasen Biotechnology Co., Ltd). The quantitative analysis of Foxp3 and Foxo1 mRNA levels was performed using a OneStep RT-PCR Kit (Qiagen, Duesseldorf, Germany). The relative mRNA levels of Foxp3 and Foxo1 were calculated using the 2^{-ΔΔCT} method with β-actin serving as an endogenous control.

M⁶A quantification

The m⁶A concentration in the total RNA of CD4⁺ T cells was measured using an m⁶A RNA Methylation Quantification Kit (Abcam, Cambridge, UK). Briefly, 200 ng total RNA sample was orderly incubated with 80 µl binding solution, 50 µl diluted capture antibody, 50 µl diluted detection antibody, and 50 µl diluted enhancer solution. Then, the absorbance of each sample was measured at 450 nm after incubation of 100 µl developer solution.

Western blot

Protein samples were extracted from cells and graft kidney tissues using RadioimmunoPrecipitation Assay (RIPA) lysis buffer (Elabscience Biotechnology Co., Ltd., Wuhan). The protein levels of WTAP, Foxp3, and Foxo1 were measured using Western blot as previously described¹⁴. Briefly, extracted protein samples were electrophoretically separated by 10% sodium dodecyl sulfate polyacrylamide gel electrophoresis (SDS-PAGE) and transferred to polyvinylidene fluoride (PVDF) membranes. Then, the membranes were orderly immersed into a blocking buffer, the primary antibodies against WTAP (#56501, Cell Signaling Technology, Danvers, MA, USA), Foxp3 (ab215206, Abcam, UK), or Foxo1 (ab179450, Abcam), and corresponding secondary antibodies. The membranes were developed using Ultra-High Sensitivity ECL Kit (GlpBio Technology, Montclair, CA, USA) and iBright imaging system (Thermo Fisher Scientific, USA).

Enzyme-linked immunosorbent assay (ELISA)

The concentrations of Interleukin-10 (IL-10), IL-4, Interferon-γ (IFN-γ), and IL-17 in the culture medium of naïve CD4⁺ T cells were detected using Human IL-10 ELISA kit, Human IL-4 ELISA kit, Human IFN-γ ELISA kit, and Human IL-17 ELISA kit. The concentrations of IL-10, IL-4, and IL-6 in serum of mice were evaluated by Mouse IL-10 ELISA kit, Mouse IL-6 ELISA kit, and Mouse IL-4 ELISA kit. All the ELISA kits were purchased from Enzyme-linked Biotechnology Co., Ltd. (Shanghai, China) according to the manufacturer's recommendations.

RNA Immunoprecipitation (RIP) and m⁶A-RIP (Me-RIP)

Following the method in a previous report¹⁵, RIP assay was conducted to assess the combination between Foxo1 mRNA and WTAP/YTH m⁶A RNA-binding protein 1 (YTHDF1)/YTHDF2/YTHDF3. Before the assay, the antibody against WTAP/YTHDF1/YTHDF2/YTHDF3 was bound with protein A/G magnetic beads (Thermo Fisher Scientific). CD4⁺ T cells were collected and lysed using mild lysis buffer. The cell lysate was then incubated with magnetic beads-antibody complex overnight at 4 °C. The RNA samples were

then eluted and purified from the immunoprecipitated. qRT-PCR was used to measure the Foxo1 mRNA level in the extracted RNA samples.

Me-RIP assay was conducted to assess the m⁶A level of Foxp3 mRNA and Foxo1 mRNA using EpiMark® N6-methyladenosine Enrichment Kit (New England Biolabs, Ipswich, MA, USA). In brief, RNA samples extracted from CD4⁺ T cells were incubated with anti-m⁶A antibody conjugated with magnetic beads overnight at 4°C. The RNA samples were eluted from the immunoprecipitated. qRT-PCR was used to measure the mRNA levels of Foxp3 and Foxo1 in the extracted RNA samples.

Polysome fractionation

After infection of Lenti-WTAP or Lenti-control, CD4⁺ T cells were treated with 100 µg/ml cycloheximide (Sigma, USA) for 10 min in a 37°C incubator. Then, the cells were washed twice with ice-cold phosphate-buffered saline (PBS) supplemented with 100 µg/ml cycloheximide. The method of cytoplasmic extract preparation was followed a previous literature¹⁶. The cytoplasmic extracts were layered onto 10–50% sucrose gradient and then subjected to centrifugation at 40,000 rpm for 2 h in 4°C condition. Gradients were fractionated by a 254 nm absorbance monitor and fraction collector (Bio-Rad, USA). Finally, the obtained fractions were analyzed by qRT-PCR detection.

Dual-luciferase reporter assay

The wild-type and mutant Foxo1 coding sequence (CDS) fragments were inserted into the luciferase report vector pGL3-Basic, respectively. Recombinant plasmids were co-transfected with plasmid pRL-TK into HEK293T cells with or without infection of Lenti-WTAP or Lenti-YTHDF1. The above plasmids and reporter gene vectors were synthesized by Sango Co., Ltd. (Shanghai, China). Subsequently, the luciferase reporter assay (Promega, USA) was conducted, and the fluorescent values of renilla plasmid were taken as the internal reference.

Mouse kidney transplantation

BALB/c and C57BL/6J mice (8-week old) were purchased from ALF Biotechnology Co., Ltd (Nanjing, China). The kidneys of BALB/c mice were transplanted into C57BL/6J mice as previously described¹⁷. Briefly, BALB/c mice were anesthetized and the left kidneys were removed and placed in heparinized saline solution. C57BL/6J mice were anesthetized and received a left nephrectomy. Then, the donor's kidney was placed in the abdominal cavity of the recipient mice. The renal arteries and renal veins of the donor's kidney were anastomosed to the abdominal aorta and vena cava of the recipient's. The donated ureter was attached to the recipient's bladder. After surgery, CD4⁺ T cells (generated from normal C57BL/6J mice) infected with Lenti-control or Lenti-WTAP were injected into C57BL/6J mice through the tail vein. Ten days later, the C57BL/6J recipient mice infected with Lenti-control ($n=6$) or Lenti-WTAP ($n=6$) were sacrificed and the blood samples, spleen tissues, and graft kidney tissues were collected. The animal experiments were performed with approval from the Ethics Committee of The First Affiliated Hospital of Zhengzhou University.

Hematoxylin-eosin (H&E) staining

Graft kidney tissues were fixed using 4% paraformaldehyde and prepared into 4-µm thick sections. H&E staining was performed on kidney sections using Haematoxylin Eosin Staining kit (Solarbio Science & Technology Co., Ltd., Beijing, China). In brief, sections were immersed in hematoxylin for 10 min and then immersed in eosin for 60 s. After washing using distilled water, the sections were sealed with neutral gum and photographed under a microscope (Olympus, Tokyo, Japan).

Immunohistochemical staining

Immunohistochemical staining was performed on kidney sections using Super Plus TM High Sensitive and Rapid Immunohistochemical Kit (Elabscience Biotechnology Co., Ltd., Wuhan, China) as previously described¹⁸. Sections were immersed in boiling Dewaxing/Antigen Retrieval Buffer for 30 min. Then, sections were incubated with SP Reagent B Peroxidase Blocking Buffer for 15 min and anti-IL-10, IL-6, or IL-4 antibody (diluted by SP Reagent G Antibody Dilution Buffer) overnight at 4°C. The next day, sections were incubated with SP Reagent C Polyperoxidase-secondary antibody for 30 min. Sections were developed with the DAB working solution and were counterstained with hematoxylin.

Statistical analyses

All data were processed with SPSS Statistics 20.0 (IBM, Armonk, NY, USA) and expressed as means ± standard deviations. *P*-value was calculated

using Student's *t*-test or one-way ANOVA. A value of *P* < 0.05 was considered statistically significant.

RESULTS

WTAP expression was positively correlated with Treg cell proportion in peripheral blood CD4⁺ T cells in TOL

GSE22229 containing gene expression data of TOL, SI, and control were downloaded. The expression profiles of 10 transcripts with the most significant changes in TOL, SI, and control groups were shown in Fig. 1A. M6A-related genes with differential expression in TOL/SI group compared to the control group were shown in Table 1. Combining the data from Fig. 1A and Table 1, WTAP, an m⁶A “writer”¹⁹, was upregulated in the blood samples of TOL and SI groups compared with those of control groups and the log₂FC(fold change) > 0. Then, TOL, IR, and HC were enrolled in our study and the whole-blood samples were collected. As shown in Fig. 1B, the proportion of CD4⁺CD25⁺Foxp3⁺ cells in the whole-blood samples was higher in the IR and TOL groups than that in the HC group, and the whole-blood samples of the TOL group exhibited the highest Treg cell ratio. Using an m⁶A RNA methylation quantification kit, we found that m⁶A concentration in peripheral blood CD4⁺ T cells was increased in the IR and TOL groups compared with the HC group (Fig. 1C). To further explore the correlation between m⁶A modification and Treg cell population, mRNA levels of several well-known m6A-related genes were detected in peripheral blood CD4⁺ T cells of HC, IR, and TOL groups. As shown in Fig. 1D, WTAP demonstrated significant changes in both IR and TOL groups, and its expression level was positively correlated with the Treg cell proportion in the peripheral blood CD4⁺ T cells of TOL groups (Fig. 1E).

WTAP overexpression promoted Treg cell differentiation and function

Next, the effect of WTAP on Treg cell differentiation and function was evaluated in vitro. Naïve CD4⁺ T cells generated from the whole-blood samples of IR were infected with Lenti-WTAP or Lenti-control and then cultured for 72 h in a Treg-inducing condition. The increase of mRNA and protein levels of WTAP (Fig. 2A) and m⁶A content (Fig. 2B) in Lenti-WTAP-infected naïve CD4⁺ T cells confirmed that Lenti-WTAP infection effectively overexpressed WTAP and enhanced m⁶A modification in CD4⁺ T cells. In response to WTAP overexpression, the mRNA and protein levels of Foxp3 (Fig. 2C) and the percentage of CD25⁺Foxp3⁺ Treg cells (Fig. 2D) were increased in CD4⁺ T cells. Meanwhile, the cytokine production dominated by Treg cells (IL-10²⁰) was enhanced while the cytokine production dominated by T helper cells (IL-4, IFN-γ, and IL-17^{21, 22}) was weakened in Lenti-WTAP-infected group (Fig. 2E). These data suggested that WTAP overexpression promoted Treg cell differentiation. To evaluate the effect of WTAP overexpression on Treg cell-mediated suppression, a CFSE-based suppression assay was performed. CFSE-labeled naïve CD4⁺ T cells were co-cultured with induced Treg cells in the presence of Lenti-control or Lenti-WTAP. As shown in Fig. 2F, WTAP-overexpressed Treg cells inhibited the proliferation of naïve CD4⁺ T cells, indicating that WTAP overexpression reinforced the suppressive activity of Treg cells.

WTAP overexpression upregulated Foxo1 protein via enhancing the translation efficiency

As reported, Foxo1 functions as the transcription factor of Foxp3, inducing Foxp3 transcription by binding to its promoter²³. The results of RIP and Me-RIP assays showed that WTAP could directly bind to Foxo1 mRNA, and Foxo1 mRNA was modified by m⁶A methylation in CD4⁺ T cells (Fig. 3A). Meanwhile, WTAP overexpression increased m⁶A methylation of Foxo1 mRNA (Fig. 3B) and upregulated Foxo1 protein without changing its mRNA level (Fig. 3C). Based on these data, we proposed a hypothesis that the

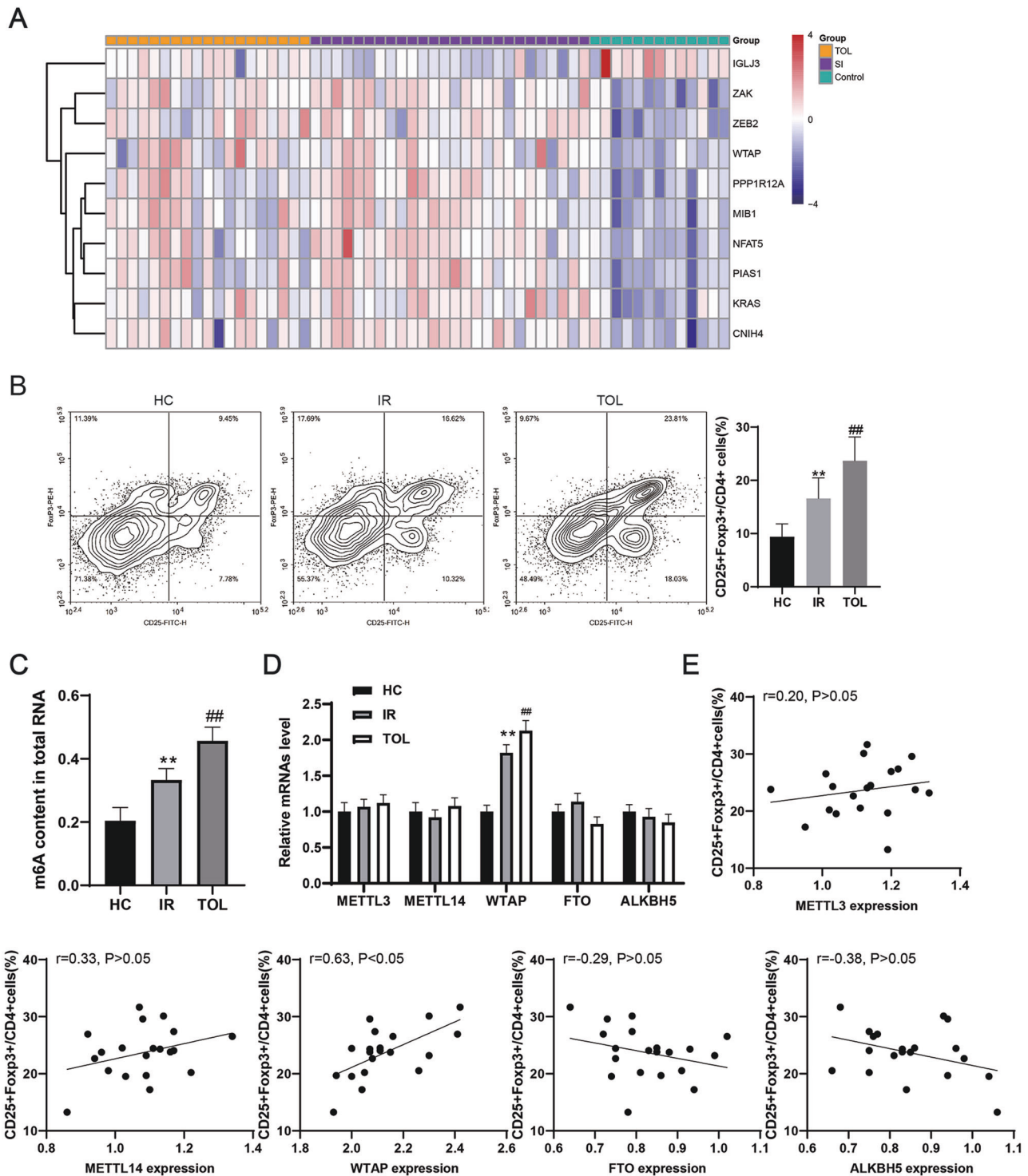


Fig. 1 Correlation between the expression of Wilms tumor 1-associating protein (WTAP) and regulatory T (Treg) cell proportion in peripheral blood CD4⁺ T cells of tolerant kidney transplant recipients (TOL). **A** The expression profiles of 10 transcripts with the most significant changes in GSE22229. Rows represent transcripts and columns represent blood samples from TOL ($n = 19$), kidney transplant recipients receiving standard immunotherapy (SI, $n = 26$), and healthy control subjects (control, $n = 13$). The color scale runs from blue (low intensity) to white (medium intensity), to red (strong intensity). **B–D** TOL ($n = 20$), IR ($n = 20$), and healthy control (HC; $n = 20$) were enrolled and the whole-blood samples were collected. CD4⁺ T cells were isolated from the whole-blood samples using dynabeads. **B** The population of CD25⁺ forkhead box P3 (Foxp3)⁺ cells in CD4⁺ T cells was measured by flow cytometry. **C** The N6-methyladenosine (m⁶A) concentration in CD4⁺ T cells was measured using an assay kit. **D** The relative mRNA levels of methyltransferase-like 3 (METTL3), METTL14, WTAP, fat mass and obesity-associated protein (FTO), and alpha-ketoglutarate-dependent dioxygenase alkB homolog 5 (ALKBH5) were measured using qRT-PCR. **E** Pearson correlation coefficient was used to determine the correlation between METTL3/METTL14/WTAP/ FTO/ALKBH5 and the proportion of CD4⁺CD25⁺Foxp3⁺ cells in the TOL group. ** $P < 0.01$ vs. HC; ## $P < 0.01$ vs. IR.

Table 1. m6A-related genes that differentially expressed in HC vs. TOL or HC vs. SI.

| Gene symbol | Full name | log ₂ FC | Type |
|-------------------|--|---------------------|---------|
| HC vs. TOL | | | |
| YTHDC1 | YTH domain containing 1 | 0.264 | readers |
| WTAP | Wilms tumor 1 associated protein | 0.312 | writers |
| IGF2BP3 | Insulin like growth factor 2 mRNA binding protein 3 | 0.608 | readers |
| HC vs. SI | | | |
| METTL3 | Methyltransferase like 3 | -0.243 | writers |
| WTAP | Wilms tumor 1 associated protein | 0.287 | writers |
| KIAA1429 | Vir like m6A methyltransferase associated | -0.205 | writers |
| RBM15 | RNA binding motif protein 15 | -0.265 | writers |
| YTHDC1 | YTH domain containing 1 | 0.219 | readers |
| HNRNPC | Heterogeneous nuclear ribonucleoprotein C | 0.153 | readers |
| ALKBH5 | α-ketoglutarate-dependent dioxygenase AlkB homolog 5 | -0.21 | erasers |
| IGF2BP2 | Insulin like growth factor 2 mRNA binding protein 2 | 0.835 | readers |

TOL = tolerant kidney transplant recipients.

SI = kidney transplant recipients receiving standard immunotherapy.

HC = healthy controls.

WTAP-mediated m6A modification of Foxo1 mRNA mainly through affecting the protein stability or translation efficiency of Foxo1. To test this, the control or WTAP overexpressed CD4⁺ T cells were treated with protein translation inhibitor cycloheximide (CHX). The western blot result revealed that WTAP overexpression had no significant effect on the stability of Foxo1 protein in CD4⁺ T cells, and the promoting effect of WTAP overexpression on Foxo1 protein did not differ from control group (Fig. 3D), excluding the possibility that WTAP regulates m6A modification through affecting Foxo1 protein stability. Thus, we speculated that the increased level of Foxo1 protein caused by m6A modification of Foxo1 mRNA mediated by WTAP might depend on the elevated translation efficiency. Next, the RNA fractions were separated by polysome profiling as follows: non-translating fraction (<40S), translation initiation fraction (including 40S ribosomes, 60S ribosomes, 80S monosomes, and < 80S) and translation active polysomes (>80S). The qRT-PCR result showed that Foxo1 mRNA in translation-active polysomes (> 80S) of CD4⁺ T cells in WTAP overexpression group were significantly higher than that in control group (Fig. 3E), supporting the hypothesis that WTAP regulates the translation and synthesis of Foxo1 protein. Collectively, these data indicated that WTAP-mediated m6A modification of Foxo1 mRNA enhanced the protein translation efficiency and thus upregulated Foxo1 protein.

WTAP enhanced Foxo1 translation efficiency depend on m6A methylation in CDS region

Using SRAMP online software to predict the m6A site of Foxo1 mRNA, we observed that the high confidence and conservative sites were in CDS region (4 sites) and 5'UTR region (1 site) (Fig. 4A). To confirm the functional m6A site, RNA from CD4⁺ T cells was processed in fragmentation and the RIP experiment was performed with m6A antibody. The result showed that overexpression of WTAP promoted m6A methylation in CDS region 2231–2291 (Fig. 4B). Since this region contains 3 possible m6A sites, we linked the Foxo1 CDS region to the polyclonal site of pGL3-basic to determine the role of each site, including the 2231 mutation (Foxo1-CDS-Mut1), 2261 mutation (Foxo1-CDS-Mut2) and 2291 mutation (Foxo1-CDS-Mut3) in Foxo1 CDS region (Fig. 4C). Using the dual-luciferase reporter fused with the CDS fragment of Foxo1, we found that the luciferase activity was significantly increased in HEK293T cells when

overexpressed WTAP, while this effect was abolished by the mutants (Fig. 4D), implying that the WTAP exert its function through the m6A sites 2231, 2261 and 2291 in Foxo1 CDS region.

Previous studies have demonstrated that YTHDF1 binds to m6A and promotes its translation efficiency^{24, 25}. We next investigated whether YTHDF1 was involved in the recognition of Foxo1 m6A site. According to the RIP experiments, the binding of YTHDF1 and Foxo1 mRNA was more significant compared with YTHDF2 and YTHDF3 (Fig. 4E). In addition, overexpression of YTHDF1 in CD4⁺ T cells had no significant effect on Foxo1 mRNA level, but markedly increased Foxo1 protein level (Fig. 4F). To estimate the specific binding site of YTHDF1 to Foxo1, the RIP assay was performed and the result showed that YTHDF1 mainly bind to CDS region 2231–2291 m6A sites (Fig. 4G). Next, the dual luciferase experiment was performed to determine the recognition efficiency of YTHDF1 on Foxo1 CDS m6A sites that has been proved to be methylated by WTAP. As shown in Fig. 4H, the effect of YTHDF1 on luciferase activity was attenuated by the mutants, indicating that YTHDF1 could recognize 2231, 2261, and 2291 m6A sites. Besides, the dual overexpressing WTAP and YTHDF1 showed the highest luciferase among the groups and it also indicated that YTHDF1 cooperated with WTAP to promote the translation efficiency. Besides, in YTHDF1 silenced CD4⁺ T cells, WTAP failed to promote Foxo1 translation (Fig. 4I). These data suggested that WTAP promoted Foxo1 translation depend on YTHDF1's recognition on CDS m6A sites.

In addition to these data, whether WTAP overexpression promoted Treg cell differentiation and function through enhancing the m6A modification of Foxo1 mRNA was evaluated. Naïve CD4⁺ T cells generated from the whole-blood samples of IR were infected with Lenti-control, Lenti-WTAP, Lenti-WTAP + Lenti-FTO (Fat mass and obesity-associated, an m⁶A demethylase), or Lenti-WTAP + Lenti-FTO + Lenti-Foxo1, and then cultured for 72 h in a Treg-inducing condition. As shown in Supplementary fig. 1A, B, FTO overexpression reduced the m⁶A modification of Foxo1 mRNA and Foxo1 protein level upregulated by Lenti-WTAP without affecting Foxo1 mRNA level, confirming that WTAP overexpression promoted Foxo1 expression by enhancing the m⁶A modification of its mRNA. While Lenti-Foxo1 infection elevated Foxo1 mRNA and protein levels without changing the m⁶A modification of Foxo1 mRNA (Supplementary fig. 1A, B). In response to Lenti-FTO infection, Foxp3 mRNA and protein levels were

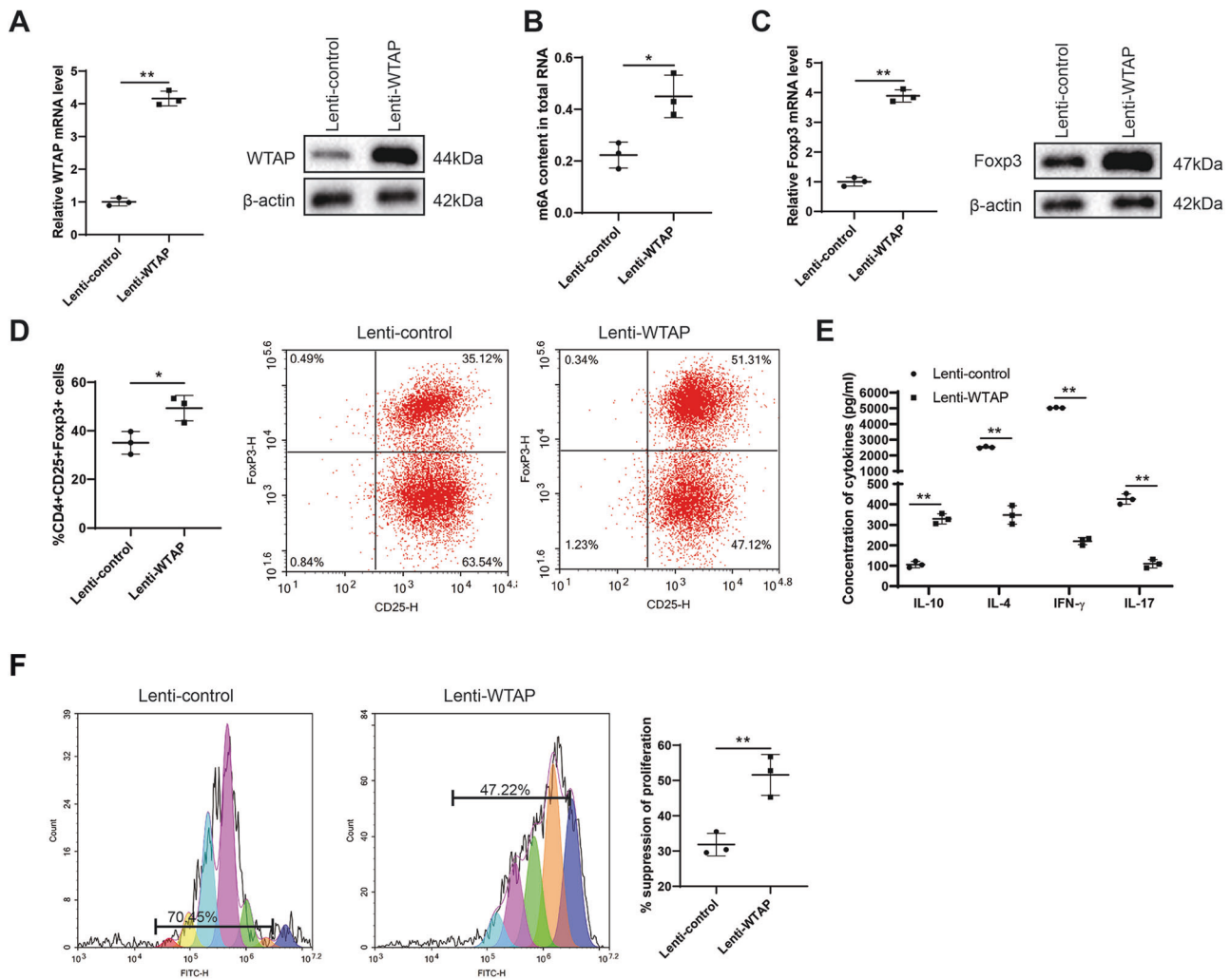


Fig. 2 The effect of WTAP overexpression on Treg cell differentiation and function. **A–E** Naïve CD4⁺ T cells generated from the whole-blood samples of IR were infected with lentivirus (Lenti)-WTAP or its negative control (Lenti-control) and then cultured for 72 h in a Treg-inducing condition. **A** The mRNA and protein levels of WTAP were examined using qRT-PCR and Western blot, respectively. β -actin was used as an internal control. **B** The m⁶A concentration was measured using an assay kit. **C** The mRNA and protein levels of Foxp3 were examined using qRT-PCR and Western blot, respectively. β -actin was used as an internal control. **D** The population of CD25⁺ Foxp3⁺ cells was measured by flow cytometry. **E** Concentrations of IL-10, IL-4, interferon- γ (IFN- γ), and IL-17 in the medium of cultured cells were detected using enzyme-linked immunosorbent assay (ELISA). **F** Carboxyfluorescein diacetate succinimidyl ester (CFSE)-labeled naïve CD4⁺ T cells were co-cultured with induced Treg cells generated from naïve CD4⁺ T cells in the presence of Lenti-control or Lenti-WTAP. The proliferation of naïve CD4⁺ T cells was analyzed by flow cytometry. * $P < 0.05$, ** $P < 0.01$ vs. Lenti-control.

decreased (Supplementary fig. 1C), the population of Treg cells was reduced (Supplementary fig. 1D), the cytokine production dominated by Treg cells were weakened (Supplementary fig. 1E), and the cytokine production dominated by T helper cells were enhanced (Supplementary fig. 1E) in CD4⁺ T cells in the presence of Lenti-WTAP, suggesting that FTO overexpression abrogated the Treg cell differentiation induced by WTAP overexpression. While the inhibitory effect of Lenti-FTO on Treg cell differentiation was removed by Lenti-Foxo1 (Supplementary fig. 1C–E). Moreover, FTO overexpression removed the Treg cell-mediated suppression of naïve T cells reinforced by WTAP overexpression, which manifested as the weakened suppressive effect of WTAP + FTO-overexpressed Treg cells on the proliferation of naïve CD4⁺ T cells compared with the WTAP-overexpressed Treg cells (Supplementary fig. 1F). Similarly, the effect of FTO overexpression on Treg cell-mediated suppression of naïve T cells was also removed by Foxo1 overexpression (Supplementary fig. 1F). Hence, we concluded that Foxo1 mediated the promoting effect of WTAP on Treg cell differentiation and function.

WTAP overexpression alleviated allograft rejection in kidney transplant model mice

CD4⁺ T cells (generated from normal C57BL/6J mice) infected with Lenti-control or Lenti-WTAP were injected into kidney transplant model mice to evaluate the effect of WTAP on kidney allograft rejection in vivo. The kidney transplant model mice treated with Lenti-control-infected CD4⁺ T cells demonstrated an acute kidney rejection, manifesting as intense inflammatory cell infiltration and renal small artery luminal stenosis, whereas this rejection was alleviated in kidney transplant model mice treated with Lenti-WTAP-infected CD4⁺ T cells (Fig. 5A). Increases in m⁶A concentration and WTAP expression in the graft kidney confirmed that Lenti-WTAP-infected CD4⁺ T cells successfully enhanced m⁶A modification and overexpressed WTAP in the kidney transplant model mice (Fig. 5B, C). In response to WTAP overexpression, Foxo1 expression was upregulated in the graft kidney (Fig. 5D), CD4⁺ T cell proportion was decreased, while CD25⁺ Foxp3⁺ cell population of total CD4⁺ T cells was increased in the spleen tissues (Fig. 5E), confirming that WTAP

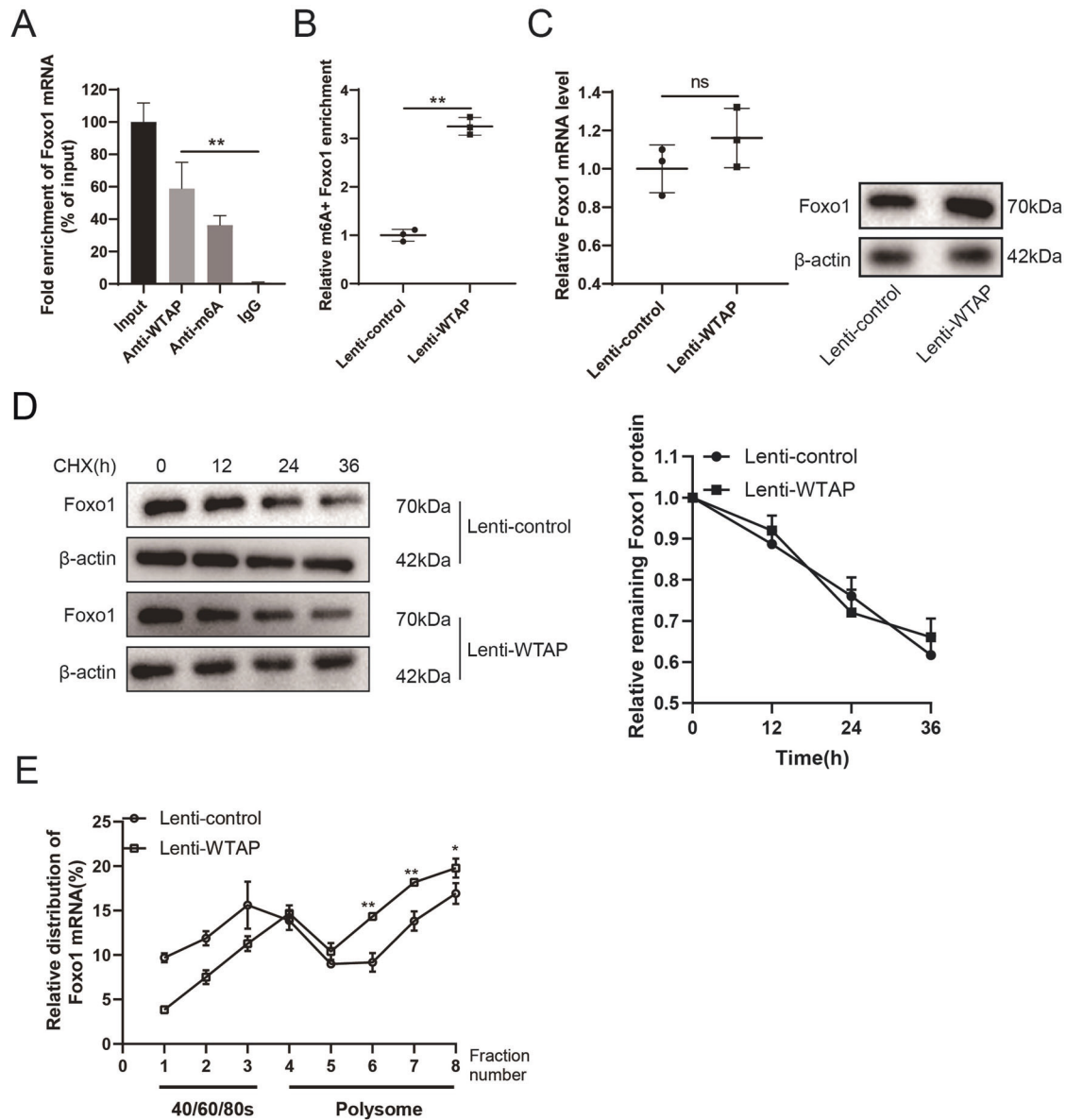


Fig. 3 The mechanism by which WTAP overexpression enhanced forkhead box other 1 (Foxo1) expression. A–E all performed on CD4⁺ T cells generated from the whole-blood samples of IR. **A** RNA Immunoprecipitation (RIP) and methylated RIP (Me-RIP) assays were performed on cells. The enrichment of Foxo1 mRNA in the products immunoprecipitated by the anti-WTAP or anti-m⁶A antibody was examined using qRT-PCR. IgG was used as a negative control. **B** Me-RIP assay was performed on cells infected with Lenti-WTAP or Lenti-control. The enrichment of Foxo1 mRNA in the products immunoprecipitated by the anti-m⁶A antibody was examined using qRT-PCR. **C** mRNA and protein levels of Foxo1 in cells infected with Lenti-WTAP or Lenti-control were measured using qRT-PCR and Western blot, respectively. β -actin was used as an internal control. **D** Cells were infected with Lenti-WTAP or Lenti-control and then treated with cycloheximide (CHX, 10 μ M) and the Foxo1 protein level was examined using Western blot at indicated time points after CHX treatment. **E** Cells were infected with Lenti-WTAP or Lenti-control, and polysome fractionation assay was conducted to measure relative distribution of Foxo1 mRNA. * $P < 0.05$, ** $P < 0.01$ vs. IgG or Lenti-control. ns not statistically significant.

overexpression was also able to promote Foxo1 expression and Treg cell differentiation in vivo. Moreover, IL-10 level was elevated, while IL-6 and IL-4 levels were lessened in the plasma and graft kidney tissues of kidney transplant model mice treated with Lenti-WTAP-infected CD4⁺ T cells (Fig. 5F, G), confirming that WTAP overexpression relieved inflammatory response in the kidney transplant model mice.

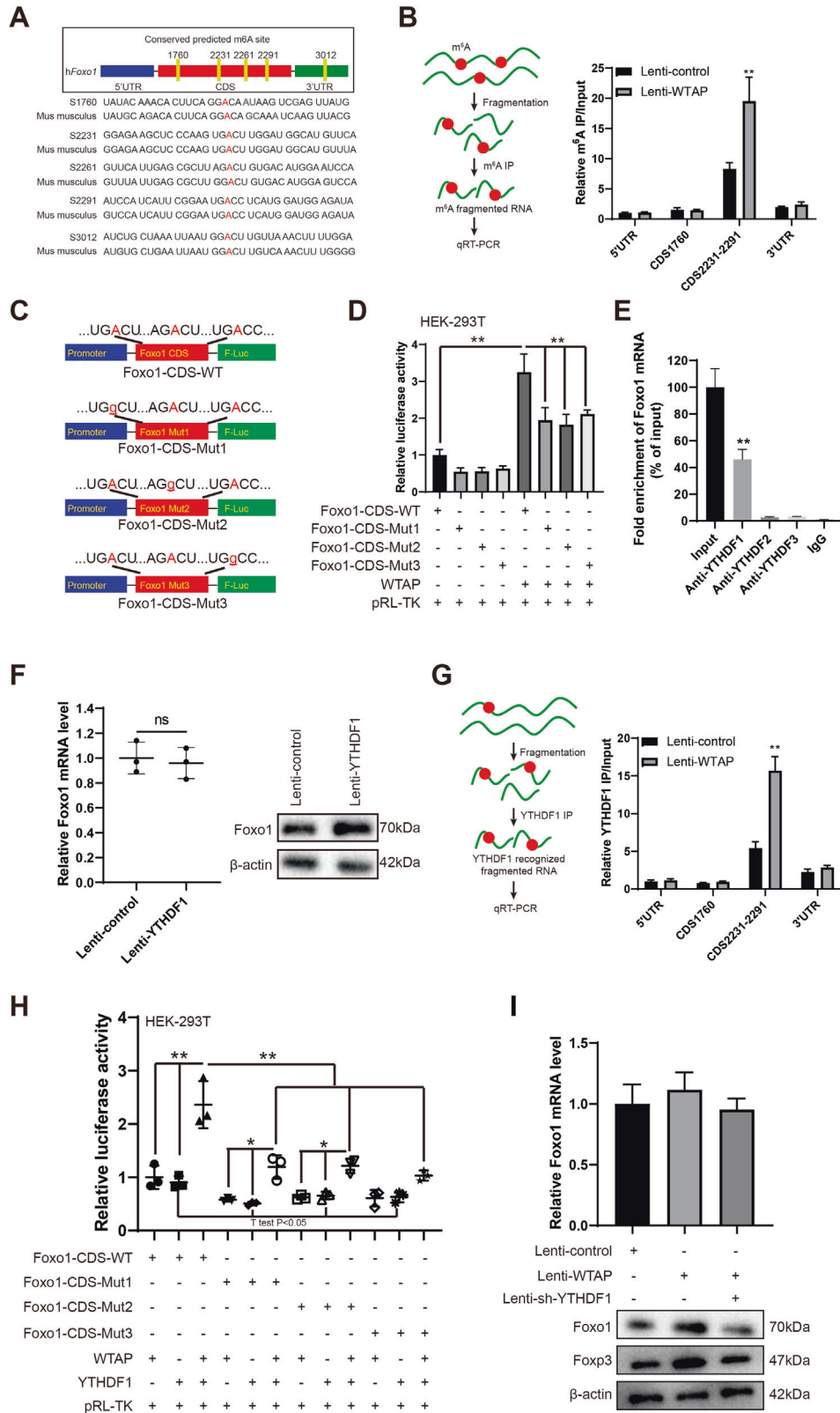
The mechanism of WTAP regulating the differentiation of regulatory T cells

In naïve CD4⁺ T cells from kidney transplant recipients with immune rejection, the elevated WTAP expression enhanced Foxo1 translation

efficiency, which depends on the YTHDF1's recognition on CDS m⁶A sites, thus upregulating Foxo1 protein level and ultimately promoting Treg cell differentiation and function (Fig. 6).

DISCUSSION

As a recent hot topic in the field of epigenetic regulation, m⁶A modification is involved in diverse biological processes, including immunoregulation¹¹. Nevertheless, the relationship between m⁶A modification and immune tolerance post kidney transplant remains unclear. In this study, we found that the m⁶A modification level was elevated in the CD4⁺ T cells of TOL. The following experiments



showed that the high level of m⁶A modification was attributed to WTAP upregulation. The highly expressed WTAP facilitated Foxo1 transcription by enhancing the m⁶A modification of Foxo1 mRNA in CDS region, which reinforced the Foxo1-mediated Foxp3 transcription and subsequent Treg cell differentiation and function.

WTAP is a subunit of the m⁶A methyltransferase complex, affecting gene expression by catalyzing the m⁶A formation in the target gene's mRNA²⁶. In recent years, studies on the biological role of WTAP mainly focus on cancer. In hepatocellular carcinoma (HCC), the high expression of WTAP results in a post-

Fig. 4 WTAP promoted Foxo1 translation depend on m6A methylation in CDS region. **A** m6A site on Foxo1 mRNA was predicted by SRAMP online software (<http://www.cuilab.cn/sramp/>). **B** RNA is processed in fragmentation and the Me-RIP assay was performed on cells. The enrichment of m6A in the products immunoprecipitated in Lenti-WTAP and Lenti-control group was examined using qRT-PCR. **C** The Foxo1 CDS region was linked to the polyclonal site of pGL3-basic, including Foxo1 CDS region 2231 mutated vector (Foxo1-CDS-Mut1), 2261 mutated vector (Foxo1-CDS-Mut2), and 2291 mutated vector (Foxo1-CDS-Mut3). Lower-case letters are the mutation sites. **D** Using the dual-luciferase reporter gene fused with the CDS fragment of Foxo1, the wild-type (WT) or mutated vectors linked to polyclonal site of pGL3-basic, containing Foxo1-CDS-WT, Foxo1-CDS-Mut1, Foxo1-CDS-Mut2, and Foxo1-CDS-Mut3 were transfected into HEK293T cells, with or without Lenti-WTAP (WTAP) infection. The luciferase activity of Foxo1 was detected. **E** RIP assay was performed to confirm the interaction between YTHDF1 /2/3 and Foxo1 mRNA. **F** CD4⁺ T cells were infected with Lenti-control or Lenti-YTHDF1, the Foxo1 mRNA and protein level was measured. β -actin was used as an internal control. **G** Me-RIP assay was performed, and the enrichment of YTHDF1 in the immunoprecipitates in Lenti-WTAP and Lenti-control group was examined by qRT-PCR. **H** The dual luciferase experiment was performed with transfections of Foxo1-CDS-WT, Foxo1-CDS-Mut1, Foxo1-CDS-Mut2, and Foxo1-CDS-Mut3, or the infections of Lenti-WTAP (WTAP) and Lenti-YTHDF1 (YTHDF1) in HEK293T cells, and the luciferase activity of Foxo1 was detected. **I** CD4⁺ T cells were infected with Lenti-control or Lenti-WTAP, or co-infected with Lenti-WTAP and Lenti-sh-YTHDF1. The mRNA and protein level of Foxo1 and Foxp3 were evaluated. β -actin was used as an internal control. * $P < 0.05$ vs. Foxo1-CDS-Mut1 + WTAP or Foxo1-CDS-Mut1 + YTHDF1 or Foxo1-CDS-Mut2 + WTAP or Foxo1-CDS-Mut2 + YTHDF1. ** $P < 0.01$ vs. IgG or Lenti-control or Foxo1-CDS-WT or Foxo1-CDS-WT + WTAP or Foxo1-CDS-WT + WTAP + YTHDF1. *ns* not statistically significant.

transcriptional suppression of ETS proto-oncogene 1 in an m⁶A-mediated manner, which reinforced the proliferation of HCC cells²⁷. During osteosarcoma tumorigenesis progression, WTAP is overexpressed and serves as an independent prognostic factor for the poor prognosis of osteosarcoma patients²⁸. However, the WTAP act as an m⁶A regulator in allograft rejection after kidney transplantation has not been explored previously. In our study, WTAP was upregulated in the CD4⁺ T cells of TOL and positively correlated with Treg cell proportion. WTAP overexpression promoted Treg cell proportion in naïve CD4⁺ T cells and reinforced Treg-mediated suppression toward naïve T cells. Consistent with our study, Li et al.²⁹ reported the regulatory effect of WTAP on immune cells. In their research, WTAP was upregulated in gastric carcinoma and its expression level was associated with T lymphocyte infiltration and immune cell production. However, differing from the previous study, our study for the first time reported the specific effect of WTAP on Treg cell proliferation and function and confirmed that WTAP overexpression partly alleviated allograft rejection in kidney transplant model mice by targeting Treg cells.

Foxp3 is a key lineage-specifying factor of Treg cells and its expression is essential for the maintenance of Treg cell function³⁰. Through repressing the Foxp3 transcription, IL-21 effectively inhibited Treg cell proliferation and differentiation, resulting in the activation of the downstream immune response and the progression of Graves' disease³¹. In our study, the increase of Foxp3 mRNA and protein levels were observed in CD4⁺ T cells when infected with Lenti-WTAP. However, WTAP overexpression failed to affect the m⁶A level of Foxp3 mRNA. Therefore, we speculated that WTAP might promote Foxp3 expression through other pathways, and consequently reinforced Foxp3-mediated Treg cell differentiation and function. Foxo1 is a member of the FOX transcription factor family. As reported, Foxo1 functions as the transcription factor of Foxp3, inducing the Foxp3 transcription by binding to its promoter²³. Of note, the research of Peng et al.³² reported that there were two adenosine sites on Foxo1 mRNA that could be methylated to m⁶A by METTL3. Besides, Jian et al.³³ reported that METTL14 was able to increase the m⁶A modification of Foxo1 mRNA, thus upregulating its expression during endothelial inflammation. These studies indicate that Foxo1 is regulated by m⁶A modification at a post-translational level. Based on these findings, we proposed a hypothesis that WTAP regulated Foxo1 expression by m⁶A modification at a post-translational level, thereby reinforcing Foxo1-mediated Foxp3 transcription. Consistent with our hypothesis, the data showed that WTAP overexpression enhanced m⁶A methylation of Foxo1 mRNA and promoted Foxo1 protein level in CD4⁺ T cells without affecting its mRNA level, indicating that WTAP could regulate Foxo1 expression through m⁶A modification. Specific m⁶A

binding proteins lead to the diverse biological functions for m⁶A modification, while YTHDF1-mediated m⁶A post-transcriptional enhancement is a typical module³⁴. For instance, Pi et al.³⁵ found that frizzled7 translation was augmented by YTHDF1 in an m⁶A-dependent manner, leading to the excessive activation of the Wnt/beta-catenin pathway in gastric carcinogenesis; Liu et al.³⁶ reported that YTHDF1 promoted eukaryotic initiation factor 3c (EIF3C) by binding to m⁶A-modified EIF3C mRNA, thereby driving the tumorigenesis of ovarian cancer. In the present study, to explore the specific m⁶A binding protein involved in the regulation of WTAP on Foxo1, a RIP assay was performed on CD4⁺ T cells. Compared with products immunoprecipitated by the anti-YTHDF2/3, the Foxo1 mRNA was detected only in the products immunoprecipitated by the anti-YTHDF1 antibody. Meanwhile, YTHDF1 overexpression upregulated Foxo1 protein in CD4⁺ T cells, further confirmed that the YTHDF1 contributed to the WTAP-reinforced Foxo1 expression. In addition, the present study demonstrated that WTAP-mediated m⁶A modification of Foxo1 mRNA through enhancing its protein translation efficiency, which is dependent on the YTHDF1's recognition on CDS region of m⁶A methylation sites. This confirmation enriches the mechanistic investigation for the regulation of WTAP on Foxo1 level, which may provide a novel insight for more comprehensive understanding of the potential mechanism.

M⁶A modification is reversible and can be erased by m⁶A demethylases³⁷. In the present study, FTO overexpression removed the promoting effect of WTAP overexpression on Foxo1 expression, Treg cell proportion, and Treg-mediated suppression toward naïve T cells, while Foxo1 overexpression reversed these trends. These data confirmed that WTAP exerted its regulatory effect on Treg cell differentiation and function by upregulating Foxo1 expression in an m⁶A-dependent manner. In addition, these data also indicated the vital role of Foxo1 in controlling Treg cell differentiation and function. This finding in our study is also supported by other previous studies. The research of Kerdiles et al.³⁸ showed that the absence of Foxo1 suppressed the development of Treg cells and those that developed were nonfunctional in vivo. Hsu et al.³⁹ found that IL-10 potentiated Treg cell differentiation through enhancing Foxo1 nuclear location. In the follow-up research work, to further clarify whether Foxo1 regulation of Treg cells is entirely dependent on Foxo1-mediated transcription activation of Foxp3, we will knockdown Foxp3 in Foxo1 overexpressed-CD4⁺ T cells, and then evaluate the Treg cell differentiation and function.

In summary, the present study confirmed that WTAP overexpression promoted Treg cell differentiation and function through enhancing m⁶A modification in Foxo1 mRNA, suggesting the positive role of WTAP in the induction of immune tolerance post kidney transplantation.

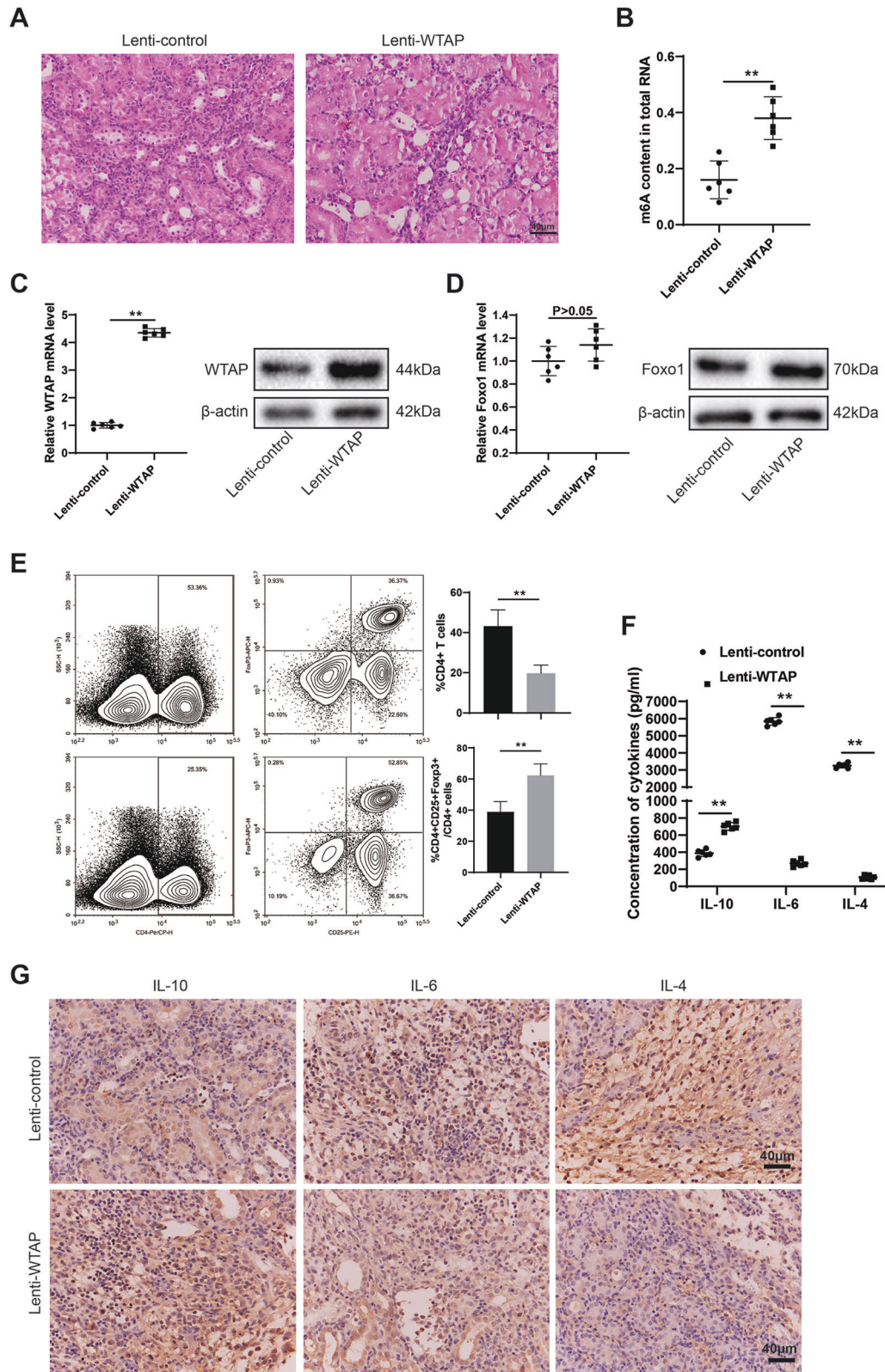


Fig. 5 The effect of WTAP overexpression on allograft rejection in kidney transplant model mice. CD4⁺ T cells (generated from C57BL/6J normal mice) infected with Lenti-control or Lenti-WTAP were injected into kidney transplant model mice through the tail vein. Ten days later, the blood samples, spleen tissues, and graft kidney tissues of mice in Lenti-control and Lenti-WTAP groups ($n = 6$ per group) were collected. **A** Hematoxylin-eosin (H&E) staining performed on graft kidney tissues of mice (Scale bar = 40 μ m). **B** The m⁶A concentration in graft kidney tissues was measured using an assay kit ($n = 6$). The mRNA and protein levels of **C** WTAP and **D** Foxo1 in the graft kidney tissues were measured using qRT-PCR and Western blot, respectively ($n = 6$). **E** The populations of CD4⁺ T cells and CD4⁺ CD25⁺ Foxp3⁺ cells in the spleen tissues were measured using flow cytometry ($n = 6$). **F** The plasma concentrations of IL-10, IL-6, and IL-4 were measured using ELISA ($n = 6$). **D** Immunohistochemical stainings for IL-10, IL-6, and IL-4 were performed on graft kidney tissues of mice (Scale bar = 40 μ m). ** $P < 0.01$ vs. Lenti-control.

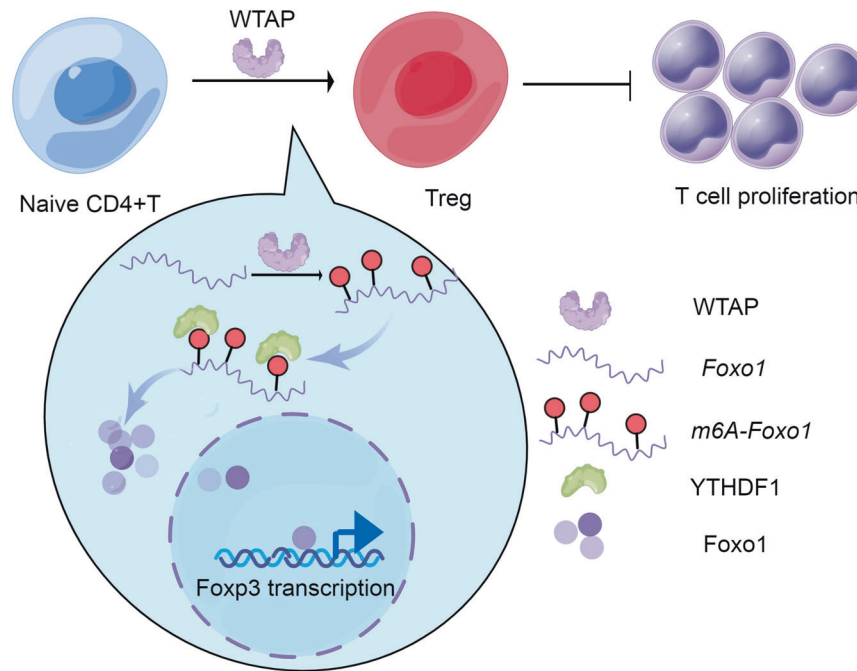


Fig. 6 Schematic diagram of WTAP affecting Treg differentiation and function. Naive CD4⁺ T cells generated from the whole-blood samples of immune rejection (IR) were cultured in Treg-inducing condition. In naïve CD4⁺ T cells, the elevated WTAP level facilitated Foxo1 translation efficiency by enhancing the m6A modification of Foxo1 mRNA in CDS region, thereby promoting the Foxo1-mediated Foxp3 transcription and Treg differentiation and function.

DATA AVAILABILITY

The datasets used and/or analyzed during the current study are available from the corresponding author on reasonable request.

REFERENCES

- Zhang R. Donor-specific antibodies in kidney transplant recipients. *Clin J Am Soc Nephrol.* **13**,182–192 (2018).
- Shrestha BM. Two decades of tacrolimus in renal transplant: basic science and clinical evidences. *Exp Clin Transpl.* **15**,1–9 (2017).
- Yu P, Xiong S, He Q, Chu Y, Lu C, Ramlogan C, et al. Induction of allogeneic mixed chimerism by immature dendritic cells and bone marrow transplantation leads to prolonged tolerance to major histocompatibility complex disparate allografts. *Immunology.* **127**, 500–511 (2009).
- Georgiev P, Charbonnier LM, Chatila TA. Regulatory T Cells: the many faces of Foxp3. *J Clin Immunol.* **39**, 623–640 (2019).
- Braudeau C, Racape M, Giral M, Louis S, Moreau A, Berthelot L, et al. Variation in numbers of CD4⁺CD25^{high}FOXP3⁺ T cells with normal immuno-regulatory properties in long-term graft outcome. *Transpl Int.* **20**, 845–855 (2007).
- Pang XL, Wang ZG, Liu L, Feng YH, Wang JX, Xie HC, et al. Immature dendritic cells derived exosomes promotes immune tolerance by regulating T cell differentiation in renal transplantation. *Aging.* **11**, 8911–8924 (2019).
- Wu H, Singer J, Kwan TK, Loh YK, Wang CM, Tan J, et al. Gut microbial metabolites induce donor-specific tolerance of kidney allografts through induction of t regulatory cells by short-chain fatty acids. *J Am Soc Nephrol.* **31**, 1445–1461(2020).
- Ono M. Control of regulatory T-cell differentiation and function by T-cell receptor signalling and Foxp3 transcription factor complexes. *Immunology.* **160**, 24–37 (2020).
- Flekens V, Minutti CM, Wu X, Wei X, Pals C, McCrae J, et al. Nemo-like kinase drives Foxp3 stability and is critical for maintenance of immune tolerance by regulatory T cells. *Cell Rep.* **26**, 3600–3612 (2019).
- He L, Li H, Wu A, Peng Y, Shu G, Yin G. Functions of N6-methyladenosine and its role in cancer. *Mol Cancer.* **18**, 176 (2019).
- Zhang C, Fu J, Zhou Y. A review in research progress concerning m6A methylation and immunoregulation. *Front Immunol.* **10**, 922 (2019).
- Tong J, Cao G, Zhang T, Sefik E, Vesely M, Broughton J, et al. m(6)A mRNA methylation sustains Treg suppressive functions. *Cell Res.* **28**, 253–256 (2018).
- Dusséaux M, Masse-Ranson G, Darche S, Ahodantin J, Li Y, Fiquet O, et al. Viral load affects the immune response to HBV in mice with humanized immune system and liver. *Gastroenterology.* **153**, 1647–1661 (2017).
- Roman, MG., Flores, LC., Cunningham, GM., Cheng, C., Allen, C. & Bai, Y. et al. Thioredoxin down-regulation in the cytosol in thioredoxin 2 transgenic mice did not have beneficial effects to extend lifespan in male C57BL/6 mice. *Aging Pathobiol Ther.* **2**, 203–209 (2020).
- Wu T-F, Liu Y, Guo X-H. CASC15 promotes lens epithelial cell apoptosis in age-related cataracts by regulating MIR-139-5p/caspase-3. *Clin Surg Res Commun.* **3**, 16–24 (2019).
- Rousseau D, Kaspar R, Rosenwald I, Gehrke L, Sonenberg N. Translation initiation of ornithine decarboxylase and nucleocytoplasmic transport of cyclin D1 mRNA are increased in cells overexpressing eukaryotic initiation factor 4E. *Proc Natl Acad Sci USA.* **93**, 1065–1070 (1996).
- Wang YY, Jiang H, Pan J, Huang XR, Wang YC, Huang HF, et al. Macrophage-to-Myofibroblast transition contributes to interstitial fibrosis in chronic renal allograft injury. *J Am Soc Nephrol.* **28**, 2053–2067 (2017).
- Lee A, Lei H, Zhu L, Jiang Z, Ladiges W. Resilience to acute sleep deprivation is associated with attenuation of hippocampal mediated learning impairment. *Aging Pathobiol Ther.* **2**, 195–202 (2020).
- Wang T, Kong S, Tao M, Ju S. The potential role of RNA N6-methyladenosine in Cancer progression. *Mol Cancer.* **19**, 88 (2020).
- Kasashima S, Kawashima A, Zen Y, Ozaki S, Kasashima F, Endo M, et al. Up-regulated interleukins (IL-6, IL-10, and IL-13) in immunoglobulin G4-related aortic aneurysm patients. *J Vasc Surg.* **67**, 1248–1262 (2018).
- Constantinescu CS, Farooqi N, O'Brien K, Gran B. Experimental autoimmune encephalomyelitis (EAE) as a model for multiple sclerosis (MS). *Br J Pharmacol.* **164**, 1079–1106 (2011).
- Talaat RM, Mohamed SF, Bassyouni IH, Raouf AA. Th1/Th2/Th17/Treg cytokine imbalance in systemic lupus erythematosus (SLE) patients: Correlation with disease activity. *Cytokine.* **72**, 146–153 (2015).
- Bothur E, Raifer H, Haftmann C, Stittrich A, Brüstle A, Brenner D, et al. Antigen receptor-mediated depletion of FOXP3 in induced regulatory T-lymphocytes via PTPN2 and FOXO1. *Nat Commun.* **6**, 8576 (2015).
- Wang X, Zhao BS, Roundtree IA, Lu Z, Han D, Ma H, et al. N(6)-methyladenosine modulates messenger RNA translation efficiency. *Cell.* **161**, 1388–1399 (2015).
- Li J, Chen K, Dong X, Xu Y, Sun Q, Wang H, et al. YTHDF1 promotes mRNA degradation via YTHDF1-AGO2 interaction and phase separation. *Cell Prolif.* **55**, e13157 (2022).
- Ping XL, Sun BF, Wang L, Xiao W, Yang X, Wang WJ, et al. Mammalian WTAP is a regulatory subunit of the RNA N6-methyladenosine methyltransferase. *Cell Res.* **24**, 177–189 (2014).

27. Chen Y, Peng C, Chen J, Chen D, Yang B, He B, et al. WTAP facilitates progression of hepatocellular carcinoma via m6A-HuR-dependent epigenetic silencing of ETS1. *Mol Cancer*. **18**, 127 (2019).
28. Chen S, Li Y, Zhi S, Ding Z, Wang W, Peng Y, et al. WTAP promotes osteosarcoma tumorigenesis by repressing HMBOX1 expression in an m(6)A-dependent manner. *Cell Death Dis*. **11**, 659 (2020).
29. Li H, Su Q, Li B, Lan L, Wang C, Li W, et al. High expression of WTAP leads to poor prognosis of gastric cancer by influencing tumour-associated T lymphocyte infiltration. *J Cell Mol Med*. **24**, 4452–4465 (2020).
30. Luo CT, Li MO. Transcriptional control of regulatory T cell development and function. *Trends Immunol*. **34**, 531–539 (2013).
31. Tan Y, Chen W, Liu C, Zheng X, Guo A, Long J. Effect of IL-21 on the Balance of Th17 Cells/Treg Cells in the Pathogenesis of Graves' Disease. *Endocr Res*. **44**, 138–147 (2019).
32. Peng S, Xiao W, Ju D, Sun B, Hou N, Liu Q, et al. Identification of entacapone as a chemical inhibitor of FTO mediating metabolic regulation through FOXO1. *Sci Transl Med*. **11**, eaau7116 (2019).
33. Jian D, Wang Y, Jian L, Tang H, Rao L, Chen K, et al. METTL14 aggravates endothelial inflammation and atherosclerosis by increasing FOXO1 N6-methyladenosine modifications. *Theranostics*. **10**, 8939–8956 (2020).
34. Chen XY, Zhang J, Zhu JS. The role of m(6)A RNA methylation in human cancer. *Mol Cancer*. **18**, 103 (2019).
35. Pi J, Wang W, Ji M, Wang X, Wei X, Jin J, et al. YTHDF1 promotes gastric carcinogenesis by controlling translation of FZD7. *Cancer Res*. **81**, 2651–2665 (2021).
36. Liu T, Wei Q, Jin J, Luo Q, Liu Y, Yang Y, et al. The m6A reader YTHDF1 promotes ovarian cancer progression via augmenting EIF3C translation. *Nucleic Acids Res*. **48**, 3816–3831 (2020).
37. Zhou Z, Lv J, Yu H, Han J, Yang X, Feng D, et al. Mechanism of RNA modification N6-methyladenosine in human cancer. *Mol Cancer*. **19**, 104 (2020).
38. Kerdiles YM, Stone EL, Beisner DR, McGargill MA, Ch'en IL, Stockmann C, et al. Foxo transcription factors control regulatory T cell development and function. *Immunity*. **33**, 890–904 (2010).
39. Hsu P, Santner-Nanan B, Hu M, Skarratt K, Lee C, Stormon M, et al. IL-10 Potentiates differentiation of human induced regulatory T Cells via STAT3 and Foxo1. *J Immunol*. **195**, 3665–3674 (2015).

AUTHOR CONTRIBUTIONS

WZ: Conceptualization, funding acquisition, data analysis; QY: data analysis, major revision; FY: Conceptualization, writing-original draft; XH & WJ & ZL: methodology, data curation; ZJ & HX: methodology, formal analysis; FG: Conceptualization, project administration; SW: Conceptualization, supervision, validation, writing-review, and editing. All authors reviewed and approved the final manuscript.

FUNDING

This study was supported by the Medical Science and Technology Research Project of Henan Province (No. SB201901004).

COMPETING INTERESTS

The authors declare no competing interests.

ETHICS APPROVAL/CONSENT TO PARTICIPATE

This study was approved by the Ethics Committee of The First Affiliated Hospital of Zhengzhou University.

ADDITIONAL INFORMATION

Supplementary information The online version contains supplementary material available at <https://doi.org/10.1038/s41374-022-00811-w>.

Correspondence and requests for materials should be addressed to Zhigang Wang, Guiwen Feng or Wenjun Shang.

Reprints and permission information is available at <http://www.nature.com/reprints>

Publisher's note Springer Nature remains neutral with regard to jurisdictional claims in published maps and institutional affiliations.